A study of gas sensing properties of ZnO nanostructures activated by UV light

M. Procek[*], T. Pustelny

Department of Optoelectronics, Silesian University of Technology, 2 Akademicka St., 44-100 Gliwice, Poland

Abstract—In this paper the response of resistance gas sensors is investigated, based on zinc oxide nanostructures to NO_2. The research is focused on the influence of ultraviolet light on the operation of such sensors at room temperature. Comparative experiment results are presented and discussed for thermal (200˚C) and UV (LED: λ=390 nm) activation in different carrier gases (air and nitrogen).

Zinc oxide (ZnO) is widely used as a gas sensing material. It can be applied in resistance and optical gas sensors to detect gases such as: NO_2, H_2, NH_3, as well as humidity and other changes [1-4]. To stabilize the operation, ZnO based sensors require activation by high temperature (≥200˚C) or by UV radiation [5]. Room temperature sensing structures of small concentrations of NO_2 are very desirable due to their low consumption of energy and potential application, such as explosives vapor detection [6,7]. Currently, the attention of researchers in the field of gas sensors is mainly focused on materials with a developed surface area, including: nanostructures of metal oxides [7,8], graphene and its compounds [9,10] carbon nanotubes [11] and other nanostructures [12].

This paper deals with a resistance gas sensor based on ZnO nanostructures. The construction of a sensor, measurement chamber and a measurement stand is presented in this work. Characterization of investigated nanostructures is also presented. The sensor response to low concentrations of NO_2 in different conditions is presented and studied. Structure responses to NO_2 are compared and discussed in two different carrier gases (air and pure nitrogen) activated by means of high temperature or UV light.

ZnO nanostructures were obtained by the chemical method which was described in our earlier paper [3]. Obtained material was deposited on an interdigital transducer (50 nm gold layer, 5μm distance and width of electrodes, substrate: 10mm×10mm Si plate with 1μm SiO_2 layer). To deposit nanostructures on the transducer, the drop coating method was used. The resulting structures were dispersed in hexane in ultrasonic bath, and then the suspension was dropped on the transducer. After the hexane had dried, a non-adhering material was removed with compressed air.

[*] E-mail: marcin.procek@polsl.pl

The morphology and distribution of nanostructures on the transducer was investigated using scanning electron microscopy (Inspect S50, FEI). The SEM image of ZnO structures deposited on the transducer is shown in Fig. 1. It can be noted that, in terms of morphology, the obtained nanostructures are a mixture of nanotubes, tenths of micrometers long and nanopowder rice-shaped.
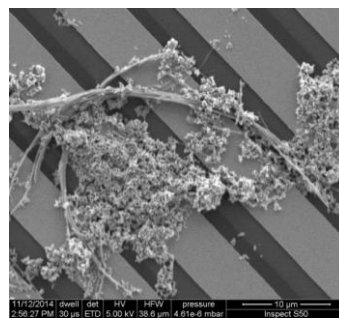

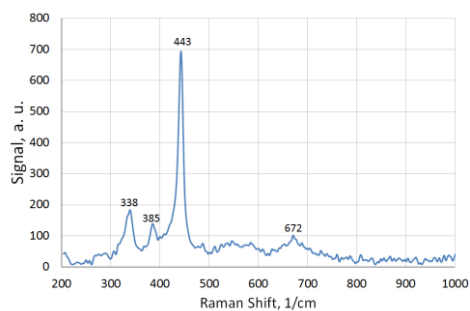Fig. 1. SEM image of ZnO nanostructures deposited on interdigital transducer.

Fig. 2. Raman spectrum of ZnO nanostructures (excitation λ=532nm).

The chemical composition was examined by means of Raman spectroscopy. In the Raman spectrum shown in Fig. 2 (NTEGRA Spectra, NT-MDT, excitation λ=532nm) peaks characteristic of ZnO nanostructures can be observed [13, 14]. That proves that the examined structures are pure ZnO nanostructures.

The prepared sensor structure deposited on the transducer was immobilized on the heater on an alumina (Al_2O_3) substrate. The heater with the structure was pasted on the chip with feedthroughs which were connected to the transducer with a gold wire (diameter 25μm) using an DELVOTEC). Temperatures of the structure were

measured by a Pt 100 temperature sensor. The chip with the sensor was covered by a measurement chamber made of the PTFE. The scheme of the chamber with the enclosed sensor is presented in Fig. 3. The chamber is equipped with a gas inlet and outlet and a quartz window (transparent to UV irradiation). As an UV light source, the LED (λ=390nm) was used.
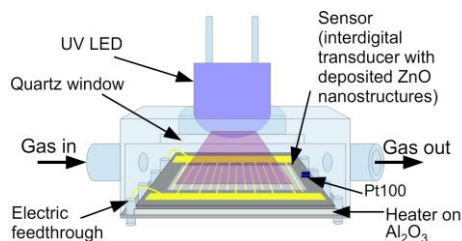

Fig. 3. Scheme of measurement chamber.

The temperature of the sensor was controlled by the PID temperature regulator (Shimaden SR 94) connected to the heater and the Pt 100 element. The resistance of the structure was monitored by the resistance meter (Agilent 34970A) connected to the PC with data acquisition software. A scheme of the measurement stand is presented in Fig. 4.
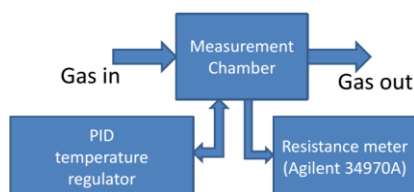

Fig. 4. Scheme of measurement stand.

The responses of the sensor to NO_2 were examined in different conditions. First, in the increased temperature (T=200˚C) in dark conditions. Next, at room temperature (T=23˚C) with UV irradiation. In all of the performed experiments, NO_2 was delivered to the measurement chamber alternatively with a clean carrier gas. Two carrier gases were used viz.: synthetic air and nitrogen, both with the relative humidity RH=6% (±1%). In all of experiments the gas flow was continuous at a rate of 500 ml/min. Concentrations of NO_2 delivered to the chamber were in the range from 1 ppm to 20 ppm.

The results obtained from the thermal activated ZnO nanostructures are presented in Fig. 5. The results in different carrier gases: air (Fig. 5a) and nitrogen (Fig. 5b) do not differ significantly. Any instability, such as abrupt changes of resistance and resistance drop thereafter, is caused by an automatic change in the measuring range of a resistance meter. The changes in the measuring ranges of the meter are unambiguous with the changes of a current source connected to the sensor - change of a current value causes rapid resistance changes and subsequent relaxation . In both cases the sensor operates properly - its response is proportional to the gas

concentration, the sorption and desorption times are comparable. The base resistance level is different (223kΩ in the air and 161kΩ in the nitrogen) due to the presence of oxygen in the air.
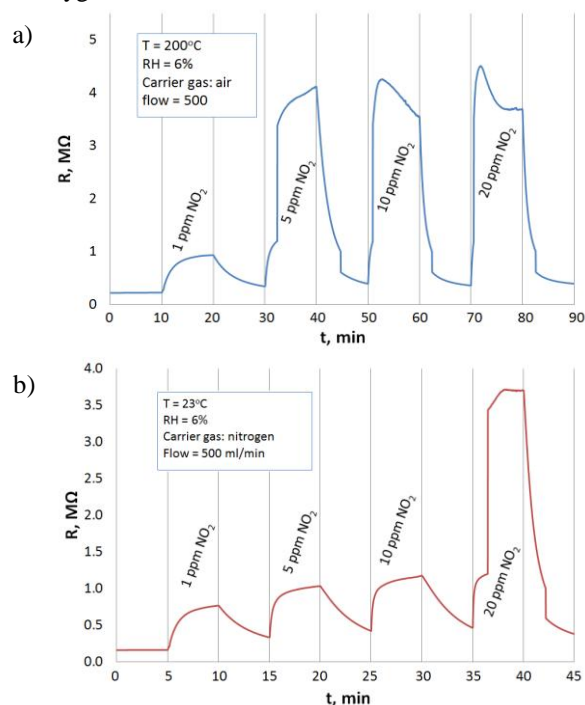

Fig. 5. Resistance changes of thermal activated (T=200˚C) ZnO nanostructures induced by NO_2 in: the air (a); and in the nitrogen (b).

The activation of ZnO nanostructures by the UV radiation causes photo-generation of charge carriers and leads to a decrease in their electrical resistance. The change of the resistance of the investigated structure after switching on the UV LED is shown in Fig. 7. When the UV illuminates the ZnO nanostructures, a very sharp drop of resistance is observed, and the sensor is ready to operate in approximately 10 seconds. In comparison, the heating of the sensor up to 200˚C and stabilization of its operation at high temperature takes a few minutes. In the case of the thermal activation the additional temperature stabilization system is required.
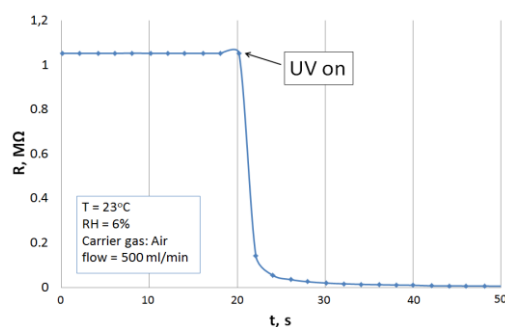

Fig. 7. Change in the resistance of ZnO nanostructures caused by UV (λ=390nm) photo-generation of charge carriers.

The results obtained by UV light activated ZnO nanostructures at room temperature are presented in Fig 8. In this case, similarly to thermal activation, the sensor operation dynamics is comparable in the air (Fig. 8a) and nitrogen (Fig. 8b) conditions. Base resistances are different in different carrier gases (5.2kΩ in the air 1.3kΩ in the nitrogen) due to the presence of oxygen in the air.
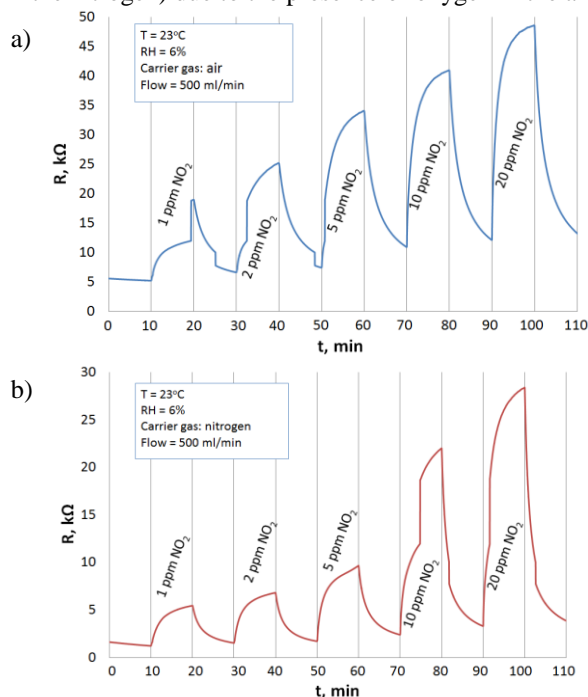

Fig. 8. Resistance response of UV (λ=390nm) activated ZnO nanostructures in the presence of NO_2 at room temperature in: the air (a); and in the nitrogen (b).

To quantitatively compare the sensor reaction to NO_2 in different conditions; a percentage sensor response was calculated: $(|R_{NO2}-R_{Base}|/ R_{Base})\cdot100\%$, where R_{NO2} is the resistance of the sensor in the presence of NO_2, and R_{Base} is the resistance in a pure carrier gas.
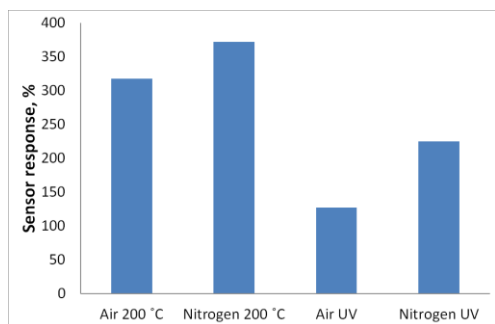

Fig. 9. Summary of sensor responses to 1ppm of NO_2 in different conditions.

Sensor responses to a 1 ppm concentration of NO_2 have been compiled in a histogram in Fig. 9 (where the spike from UV in air conditions - Fig. 8a, is neglacted). It is clearly visible that the sensor responses in the case of

thermal activation are higher than in the case of UV activation. Also the presence of oxygen in the carrier gas causes a decreasein the sensor response. This is due to the oxidasing character of both NO_2 and O_2 and their competitive adsorption on the same centers of adsorption on ZnO crystallites. The sensor responses for 1 ppm of NO_2 are higher than 100% in all the studied cases. This allows for the assumption that the sensor can detect much lower concentrations of NO_2 (at a level of pbbs).

It can be assumed that the elaborated sensor reacts to very low concentrations of NO_2 in different conditions. Higher responses are observed in the case of thermal activation of the ZnO nanostructures (in 200˚C), The dynamicity of the sensor, however, is comparable for both activation methods (thermal and UV). It has to be pointed out that in the case of UV activation, the sensor operates at room temperature, which is a very important advantage. Therefore the UV activation of the sensor requires less energy to operate. In the case of UV activation the sensor is ready to operate much faster (in about 10s) than in the case of thermal activation (in a few minutes). The lower limit of NO_2 detection of the investigated structure is much smaller than 1 ppm. The presence of oxygen in the gas mixture decreases the response to NO_2 of the sensor but it does not interfere with its proper operation. Thus the sensor activated by UV light can operate in the air at room temperature, which makes it more attractive for practical applications.

References

[1] R.K. Sonker, S.R. Sabhajeet, S. Singh, B.C. Yadav, Mat. Lett. **152**, 189 (2015).
[2] M. Procek, T. Pustelny, A. Stolarczyk, E. Maciak, Bull. Pol. Acad. Sci. Tech.Sci. **62**(4), 635 (2014).
[3] T. Pustelny *et al.,* Bull. Pol. Acad. Sci. Tech.Sci. **60**(4), 853 (2012).
[4] M.A. Borysiewicz *et al.,* Mat. Res. Soc. Symp. Proc. **1494**, 71 (2013).
[5] H. Chen, Y. Liu, C. Xie, J. Wu, D. Zeng and Y. Liao, Cera. Inter. **38**, 503 (2012).
[6] Z. Bielecki *et al.,* Metrol. Meas. Syst. **19**, 3 (2012).
[7] M. Procek, A. Stolarczyk, T. Pustelny, E. Maciak, Sesnors **15**(4), 9563 (2015).
[8] J.H. Lee, Sens. Actuators B Chem. **140**(1), 319 (2009).
[9] T. Pustelny *et al.,* Bull. Pol. Acad. Sci. Tech.Sci. **61**(2), 293 (2013).
[10] S. Derwniak, T. Pustelny, R. Muzyka, G. Konieczny, P. Kałużyński, Phot. Lett. Poland **6**(4), 130 (2014).
[11] A.D. Dobrzańska-Danikiewicz *et al.,* Phys. Stat. Soli. B, **251**(12), 2426 (2014).
[12] T. Pustelny, J. Ignac-Nowicka, B. Jarzabek, A. Burian, Optica Appl. **34**(4), 551 (2004).
[13] Z.W. Dong, C.F. Zhang, H. Deng, G.J. You, S.X. Qian, Mate. Chem. Phys. **99**(1), 160 (2006).
[14] C.F. Windich Jr., G.J. Exarhos, Ch. Yao, L.Q. Wang, Jour. Appl. Phys. **101,** 123711 (2007).